forests

MDPI

Article

Valorization of Wood Residues from Vegetation Suppression during Wind Energy Plant Implementation and Its Potential for Renewable Phenolic Compounds through Flash Pyrolysis: A Case Study in Northeast Brazil's Semi-Arid Region

Marcela Cristina Pereira dos Santos Almeida [1], Janduir Egito da Silva [2], Willame Gomes da Silva Batista [2], José Luiz Francisco Alves [2,3], Dulce Maria de Araújo Melo [2], Alexandre Santos Pimenta [1,*] and Renata Martins Braga [1,2]

[1] Graduate Program in Forest Sciences (PPGCFL), Agricultural School of Jundiaí (EAJ), Federal University of Rio Grande do Norte, Macaíba 59280-000, RN, Brazil; marcelacpsantos@hotmail.com (M.C.P.d.S.A.); renatabraga.r@gmail.com (R.M.B.)

[2] Environmental Technology Laboratory (LabTam), Primary Processing and Reuse of Produced Water and Residues Center (NUPPRAR), Federal University of Rio Grande do Norte, Natal 59075-000, RN, Brazil; janduir.egito@gmail.com (J.E.d.S.); willame_g@hotmail.com (W.G.d.S.B.); joseluiz@cear.ufpb.br (J.L.F.A.); dulce.melo@ufrn.br (D.M.d.A.M.)

[3] Department of Renewable Energy Engineering, Federal University of Paraíba, João Pessoa 58051-900, PB, Brazil

* Correspondence: alexandre.pimenta@ufrn.br

Abstract: In the past few years, wind power has become a viable alternative in Brazil to diversify the energy mix and mitigate pollutant emissions from fossil fuels. Significant wind energy generation potential is inherent in the Brazilian Northeast state of Rio Grande do Norte, due to prevailing strong winds along the coastline and elevated regions. However, clean and renewable wind energy may lead to potential biodiversity impacts, including the removal of native vegetation during plant construction and operation. This case study explores the flash pyrolysis-based valorization of three commonly suppressed species, namely *Cenostigma pyramidale* (CP), *Commiphora leptophloeos* (CL), and *Aspidosperma pyrifolium* (AP), in a wind farm situated within the Mato Grande region of Rio Grande do Norte State. The study centers on determining their bioenergy-related properties and assessing their potential for producing phenolic-rich bio-oil. The investigation of three wood residues as potential sources of high-value chemicals, specifically phenolic compounds, was conducted using a micro-furnace type temperature programmable pyrolyzer combined with gas chromatography/mass spectrometry (Py–GC/MS setup). The range of higher heating values observed for three wood residues was 17.5–18.4 MJ kg^{-1}, with the highest value attributed to AP wood residue. The bulk density ranged from 126.5 to 268.7 kg m^{-3}, while ash content, volatile matter content, fixed carbon content, and lignin content were within the respective ranges of 0.8–2.9 wt.%, 78.5–89.6 wt.%, 2.6–9.5 wt.%, and 19.1–30.6 wt.%. Although the energy-related properties signifying the potential value of three wood residues as energy resources are evident, their applicability in the bioenergy sector can be expanded via pelleting or briquetting. Yields of phenolic compounds exceeding 40% from the volatile pyrolysis products of CL and AP wood residues at 500 °C make them favorable for phenolic-rich bio-oil production. The findings of this study endorse the utilization of wood residues resulting from vegetation suppression during the installation of wind energy plants as potential feedstocks for producing bioenergy and sustainable phenolic compounds. This presents a solution for addressing a regional environmental concern following the principles of green chemistry.

Keywords: plant suppression; biomass valorization; caatinga; flash pyrolysis; phenolic compounds

check for updates

Citation: Almeida, M.C.P.d.S.; Silva, J.E.d.; Batista, W.G.d.S.; Alves, J.L.F.; Melo, D.M.d.A.; Pimenta, A.S.; Braga, R.M. Valorization of Wood Residues from Vegetation Suppression during Wind Energy Plant Implementation and Its Potential for Renewable Phenolic Compounds through Flash Pyrolysis: A Case Study in Northeast Brazil's Semi-Arid Region. *Forests* **2024**, *15*, 621. https://doi.org/10.3390/f15040621

Academic Editor: František Kačík

Received: 2 December 2023
Revised: 27 December 2023
Accepted: 5 January 2024
Published: 29 March 2024

1. Introduction

International efforts to realize Sustainable Development Goals (SDGs), particularly SDG 7 for universal access to "Affordable and Clean Energy", center on ensuring reliable, sustainable, modern, and affordable energy access for all, with an emphasis on renewable, efficient, and non-polluting energy sources [1,2]. Also, a decline in the accessibility of non-renewable energy, comprising oil and its derivatives, natural gas, coal, and uranium, was induced by the Russia–Ukraine conflict [3,4]. Hence, a substantial challenge is posed to countries pursuing resource sustainability, ensuring that technological and economic advancements result in diminished environmental impacts and enhance population well-being and social equity [5,6]. The expansion of electric energy sources, encompassing wind and solar power, and the proliferation of biomass and biodiesel resources has propelled Brazil's position in renewable energy to global eminence [7].

The emergent growth of the wind energy sector is attributed to the benefits derived from Brazil's predominant shift toward clean energy sources. Brazil's gross wind power potential, estimated at a minimum of 143 GW, considers wind speeds greater than or equal to 7 m s^{-1}, excluding offshore generation possibilities. The majority of this potential (52.3%) is concentrated within the Northeast region, with the state of Rio Grande do Norte being particularly distinguished for its substantial wind energy potential [8]. However, it is crucial to underscore that, during the deployment of wind farms, various activities are undertaken that give rise to adverse environmental consequences in the region, including vegetation suppression, road construction, soil vibration, visual disturbances, electromagnetic interference, acoustic pollution, and the potential for wildlife accidents [9,10]. The growth of renewable energy production from wind farms should not result in substantial environmental harm or compromise environmental objectives [2]. New projects must align with biodiversity protection and conservation objectives, which are in accordance with SDG 15 (Life on Land), focusing on the conservation, restoration, and sustainable use of terrestrial ecosystems [6].

Wind farms are predominantly situated in the northeastern semi-arid region of Brazil, where the Caatinga biome prevails, owing to its attractive attributes, including its strategic positioning for capturing robust and consistent wind resources alongside low and erratic rainfall patterns [9,11]. Nevertheless, despite substantial investments in this area, limited research has addressed the valorization of wood residues resulting from vegetation suppression in this region. Unfortunately, the suppressed biomass (trees, shrubs, stumps, roots, etc.) resulting from wind energy plant implementation is a neglected lignocellulosic resource with no established current use, and the lack of adequate management contributes to an increased fire risk. Common disposal methods for suppressed biomass include open-field burning or their utilization as firewood for domestic cooking by local communities. On the other hand, germplasm extraction and subsequent replanting in different areas to offset damage is integral in mitigating deforestation-induced environmental impacts. Thus, the collection of seeds and seedlings in the area to be deforested, as well as their planting in locations selected by the environmental management of the wind energy project, significantly contributes to reducing the loss of genetic diversity in the plant species of the environment [12,13]. Nevertheless, a knowledge gap exists concerning using wood and forest biomass from this region. Despite studies on the environmental consequences of vegetation removal in wind farm installation zones, there remains a dearth of specific research addressing the potential and application of this raw material.

While recent technological advancements in bioenergy generation have been noteworthy, the imperative to enhance the availability of low-cost solid raw materials and their adequate conversion in existing thermochemical conversion technologies has become a prominent concern within the bioenergy sector [14,15]. In this regard, lignocellulosic biomass derived from suppressed vegetation can represent a low-cost raw material for bioenergy production possessing a reasonable carbon content. Still, this source of lignocellulosic biomass does not exert an adverse influence on potential crop fields designated for food production, a critical consideration within agricultural economies such as Brazil. An alternative approach for the conversion of lignocellulosic biomass from suppressed vegetation into biofuels and renewable chemicals is provided by pyrolysis. Within the pyrolysis process, carbonaceous feedstocks are thermally decomposed within an oxygen-depleted environment, leading to the production of condensable vapors (bio-oil), non-condensable gases (pyrolytic gas), and carbonaceous solids (biochar). These resulting products can be utilized as biofuels and as a source of renewable chemicals [16,17].

Within the array of thermochemical conversion technologies, pyrolysis distinguishes itself from gasification and combustion through its lower operating temperature, simple operation, minimal emission of polluting gases, and reasonable cost, positioning it as a highly promising conversion method [18,19]. The yield of pyrolysis products is influenced by the heating rate applied to the biomass. To maximize the production of condensable vapors (bio-oil), high heating rates and maintenance of residence times of only a few seconds are preferred [20,21]. Also, producing renewable chemicals from wood residues generated through vegetation suppression via flash pyrolysis aligns with the fundamental principles of green chemistry, which advocate deriving chemical products from feedstocks originating from renewable resources or abundant waste materials [22]. The analytical pyrolyzer, coupled with a gas chromatograph/mass spectrometer (Py–GC/MS setup), offers a precise and well-controlled platform for identifying and quantifying volatile reaction products generated during the flash pyrolysis of lignocellulosic biomass [23,24]. This advanced coupled microscale technique applies high heating rates to samples, ensuring precise temperature control, rapid analysis, and minimal sample consumption [25,26]. As per the author's current understanding, a relevant gap in the literature concerning studies related to the valorizing wood residues resulting from vegetation suppression during the establishment of wind energy plants as raw materials for producing bioenergy and renewable chemicals.

A window of opportunity for advancing this research emerged from the imperative to capitalize on abundant, low-cost lignocellulosic biomass resources represented by suppressed species. The scope of this case study is to exploit the untapped potential of wood residues resulting from vegetation suppression during the establishment of a wind energy plant in the Mato Grande region of Rio Grande do Norte State, intending to produce bioenergy and renewable chemicals. Hence, this study makes an important contribution to the current state of knowledge by examining the flash pyrolysis of native species from the caatinga biome, colloquially known as "catingueira" (*Cenostigma pyramidale* (Tul.) E. Gagnon & G. P. Lewis), "imburana' (*Commiphora leptophloeos* (Mart.) J. B. Gillett), and "pereiro" (*Aspidosperma pyrifolium* Mart. & Zucc.). In brief, this case study has dual objectives. Firstly, the physicochemical characterization of wood residues from the three suppressed species was conducted, encompassing proximate analysis, thermogravimetric analysis, heating value, bulk density, and lignocellulosic compositional analysis to evaluate their bioenergy potential. Secondly, the study aimed to assess the potential for producing renewable phenolic compounds from the wood biomass of the three suppressed species, analyzing the composition of volatile reaction products released during flash pyrolysis using a Py–GC/MS setup. The findings of this case study are of great significance as they can assist in establishing a sustainable approach for valorizing wood residues resulting from vegetation suppression, with the potential to contribute to several SDGs proposed by the United Nations in 2015, particularly those associated with clean energy, innovation, climate change mitigation, and sustainable natural resource utilization, including Affordable and Clean Energy (SDG 7), Industry, Innovation and Infrastructure (SDG 9), Climate Action (SDG 13), and Life on Land (SDG 15).

2. Materials and Methods

The current case study is grounded in data shared by the environmental consulting firm CRN Bio Ambiental e Arqueologia pertaining to the implementation of a wind energy project. The execution of environmental activities during the establishment of the wind complex in the Mato Grande, Rio Grande do Norte, was undertaken by this firm. Additional information about establishing the wind complex is available in the

Supplementary Materials. The study's starting material comprised non-uniform-sized sawdust obtained during chainsaw cutting of aboveground wood residue derived from vegetation suppression during the installation phase of a wind energy plant. The selection of the three indigenous species—*Cenostigma pyramidale* (CP), *Commiphora leptophloeos* (CL), and *Aspidosperma pyrifolium* (AP)—was based on their higher frequency and abundance within the project area. After collecting sawdust from aboveground wood residues of each of the three indigenous species, the material underwent individual screening using a mechanical sieve shaker equipped with a 100-mesh screen, producing uniform particles with a size of approximately 0.150 mm. Subsequently, drying was carried out in an oven at 100 °C for 24 h to remove external moisture. The material obtained for each species was promptly sealed in airtight zip-lock plastic bags for subsequent use in physicochemical characterization and pyrolysis experiments.

2.1. Procedures for Conducting the Physicochemical Characterization Analyses

The proximate analysis of each wood residue was determined gravimetrically using a muffle furnace model 7000 (EDG Equipamentos, São Carlos, Brazil) to ascertain the mass percentages of inherent moisture, volatile matter, and inorganic matter (ash) based on the ASTM standard methods E871-82 [27], E872-82 [28], and E1755-01 [29], respectively. The fixed carbon content was determined through mass balance, computed as the difference between 100 wt.% and the sum of mass percentages of inherent moisture, volatile matter, and ash [30]. The mass percentages of cellulose and hemicellulose were determined through acid detergent fiber (ADF) and neutral detergent fiber (NDF) tests, as per the methodology described by Van Soest et al. [31], with minor modifications. The determination of the mass percentage of lignin was carried out following the Klason method [30]. Determining bulk density (or bulk-specific weight) for each wood residue involved measuring the mass of the sample occupying a predefined volume within a graduated cylinder, following the standard method outlined in ASTM E873-82 [32]. The determination of the higher heating value (HHV) for each wood residue was conducted using an automatic isoperibol calorimeter model 6400 (Parr Instrument Company, Moline, IL, USA), following the standard method outlined in ASTM E711 [30]. The thermal decomposition behavior of each wood residue was conducted utilizing a Q500 thermogravimetric analyzer (TA Instruments, New Castle, DE, USA) under the following operational parameters: atmospheric pressure, a nitrogen gas flow rate of 50 mL min^{-1} (with 99.999% purity), an approximate sample mass of 10 mg, an employed heating rate of 10 °C min^{-1}, and a temperature range for the reaction from 30 to 900 °C. The chemical composition of inorganic matter (ash) derived from each wood residue was determined using X-ray fluorescence (XRF) spectroscopy with a spectrometer model EDX-720 (Shimadzu, Tokyo, Japan). Triplicate measurements were performed for each physicochemical characterization analysis, and the presented data represent the mean values.

2.2. Procedure for Micro-Scale Flash Pyrolysis Experiments

Flash pyrolysis of each wood residue was performed using an analytical pyrolyzer model Pyroprobe 5200 HP-R (CDS Analytical, Oxford, MS, USA). A 1 mg pre-weighed amount was introduced into the central region of a quartz tube, with small sections of glass wool positioned at both tube ends. The analytical pyrolyzer contains an electrically heated platinum sample holder/filament, where each biomass sample underwent complete pyrolysis at a pre-defined final temperature of 500 °C, with a heating rate of 10 °C ms^{-1}, followed by an isothermal hold for 20 s. The volatile reaction products escaping from the analytical pyrolyzer were carried by Grade 5.0 nitrogen at a flow rate of 50 mL min^{-1}, which also served to maintain an inert atmosphere, and directed towards a Tenax trap possessing a 20:35 mesh (Scientific Instruments Services, Ringoes, NJ, USA). Following trapping, the volatile reaction products were desorbed at 300 °C and subsequently transferred through a heated transfer line into a gas chromatograph 3900 (Varian, Walnut Creek, CA, USA), featuring an ion trap mass spectrometer model Saturn 2100T (Varian, Walnut Creek, CA, USA) in order to characterize the nature of resulting volatile reaction products from flash pyrolysis of each biomass sample. The transfer line was consistently held at 300 °C to inhibit the condensation of lightweight volatile reaction products, and the injection port was maintained at the same temperature.

Chromatographic separation of volatile reaction products was accomplished on a fused silica capillary column, VF-5 ms model, 30 m × 0.25 mm (i.d.) × 0.1 μm (Agilent Technologies, Santa Clara, CA, USA), with Grade 5.0 helium as the carrier gas at a flow rate of 1 mL min^{-1}. The GC operated in split mode with a 1:50 ratio, utilizing a split injector at an inlet port temperature of 300 °C. The chromatographic column's heating procedure for separating volatile reaction products comprised the following: (i) holding at an initial temperature of 40 °C for 2 min; and (ii) subsequently ramping the temperature to 280 °C at a rate of 10 °C min^{-1}, with a 10 min hold. The operational parameters utilized in the Py-GC/MS setup were delineated in accordance with a document previously published by the LabTam/UFRN research team [30]. The identification of condensable volatile products was achieved through a comparison of their mass spectra with those in the NIST Mass Spectral library, with a focus on analyzing spectral similarity and assessing a similarity criterion that needed to exceed 85%. Semi-quantitative quantification of volatile reaction products in terms of relative concentration was achieved by determining absolute peak areas through the integration method. Triplicate analytical flash pyrolysis experiments were conducted to ensure sufficient experimental repeatability, and the results were presented as the mean value along with the standard deviation.

3. Results and Discussion

3.1. Physicochemical Characterization Results for Wood Residues

Table 1 presents the physicochemical properties of three wood residues, encompassing proximate composition, heating values, lignocellulosic composition, bulk density, and the chemical composition of ash, which assume significance due to their close association with the bioenergy potential of the investigated lignocellulosic residues. In the literature, the suitability of solid biofuels for thermochemical conversion is typically recognized when their moisture content is below or close to 10.0 wt.% [33]. Acceptable moisture levels (below 10.9 wt.%) are observed in the three wood residues for their application in thermochemical conversion processes, as higher moisture values indicate the necessity of drying and present challenges for the ignition and combustion of biomass.

Table 1. Physicochemical characterization results for the three wood residues subjected to proximate composition, heating values, bulk density, and lignocellulosic composition determinations.

	Aspidosperma pyrifolium	*Cenostigma pyramidale*	*Commiphora leptophloeos*
Proximate composition (wt.%)			
Moisture	7.11 ± 0.13	10.04 ± 0.06	10.85 ± 0.06
Volatile matter	89.57 ± 1.37	79.40 ± 0.26	78.50 ± 1.81
Fixed carbon	2.55 [a]	9.45 [a]	7.81 [a]
Ash	0.77 ± 0.15	1.20 ± 0.10	2.84 ± 0.11
Lignocellulosic composition (wt.%)			
Hemicellulose	11.34	19.79	13.48
Cellulose	42.64	39.03	46.26
Lignin	29.76	19.11	30.61
Heating values (MJ kg^{-1})			
HHV	18.39 ± 0.64	17.47 ± 0.20	17.99 ± 0.01
LHV	17.58	16.66	17.18
Bulk density (kg m^{-3})	268.70 ± 0.61	237.10 ± 0.10	126.50 ± 0.17
Chemical composition of ash (wt.%)			
CaO	65.33	80.12	37.61
K_2O	32.45	18.78	57.59
Fe_2O_3	2.03	--	2.34
SiO_2	--	--	1.66
Others	0.36	1.11	0.80

[a] Calculated by difference.

The proximate composition, as shown in Table 1, reveals that the AP wood residue exhibits a greater volatile matter content compared to that of the CP and CL wood residues. This observation suggests that the AP wood residue is characterized by a higher propensity for volatile product release during pyrolysis, thus favoring the production of renewable chemicals. Concerning fixed carbon, the CP and CL wood residues, with values ranging from 7.8 to 9.5 wt.%, align with the typical composition range of biomass fuels reported in the literature (66–85 wt.%) [34]. Concerning fixed carbon, the CP and CL wood residues, with values ranging from 7.8 to 9.5 wt.%, align with the typical composition range of biomass fuels reported in the literature (7–20 wt.%) [35]. A low ash content below 2.9 wt.% was observed in the three wood residues, indicative of their suitability for bioenergy applications. The presence of inorganic matter (ash) in wood residues is limited, thereby mitigating potential operational issues, such as corrosion and fouling, during the thermochemical conversion and ensuring adequate efficiency in bioenergy production. The inorganic content of the three wood residues aligns with the reported range for commercial lignocellulosic biomass fuels (0.6–9.8 wt.%) [34].

As indicated in Table 1, cellulose contents in CL and AP wood residues were higher and closely approximated at 46.26 wt.% and 42.64 wt.%, respectively, with the lower content of 39.03 wt.% observed in CP wood residue. The cellulose mass contents align well with those observed in hardwood biomasses (43–47 wt.%) [36]. The hemicellulose contents in AP and CL wood residues were closely approximated at lower levels, measuring 11.34 wt.% and 13.48 wt.%, respectively, while CP wood residue exhibited the highest content at 19.79 wt.%. The hemicellulose mass content in CP wood residue aligns closely with the range observed in hardwood biomasses (16.8–18.7 wt.%) [37]. Typical volatile reaction products from the thermal decomposition of cellulose and hemicellulose include short-chain oxygenated compounds, acetic acid, furan derivatives, ketones, and a small content of hydrocarbons [38–40]. Lignin contents ranged from 19.1 to 30.6 wt.%, with the highest observed in CL wood residue. The lignin content in the three wood residues closely matches the published range for wood species found in the Brazilian semi-arid region (23.7–32.8 wt.%), according to the literature [41]. High-lignin biomass is proposed to generate a condensable pyrolysis product (bio-oil) rich in phenolic compounds. Thus, wood residues from suppressed native species hold significant potential for producing valuable renewable chemicals (phenolic compounds) through flash pyrolysis.

Figure 1 illustrates the temperature-dependent mass loss and rate of mass loss profiles recorded during the thermal decomposition of three wood residues. The initial stage of mass loss, occurring below 100 °C, primarily involves the evaporation of inherent moisture, with an average mass loss below 10 wt.% observed in the three wood residues, consistent with the inherent moisture content indicated in the proximate composition (Table 1). The prevalent mass loss stage, occurring between 100 °C and 400 °C, is characterized by the predominant release of volatile matter, corresponding to the simultaneous devolatilization of hemicellulose and cellulose with a smaller contribution from lignin. This assertion is plausible, as the literature commonly attributes the temperature ranges of 240–325 °C and 325–400 °C to the thermal decomposition of hemicellulose and cellulose, respectively [42,43], while lignin undergoes continuous and gradual thermal decomposition over a broad temperature range spanning approximately 180–700 °C [44,45]. On average, the three wood residues exhibit an approximate 60 wt.% mass loss in this prevalent stage, aligning with the reported mass losses for the prevalent stage of wood species in the Brazilian semi-arid region [41]. At the final temperature of 900 °C, an average remnant mass below 10 wt.% was observed for three wood residues, consistent with the findings of proximate analysis (sum of fixed carbon and ash content).

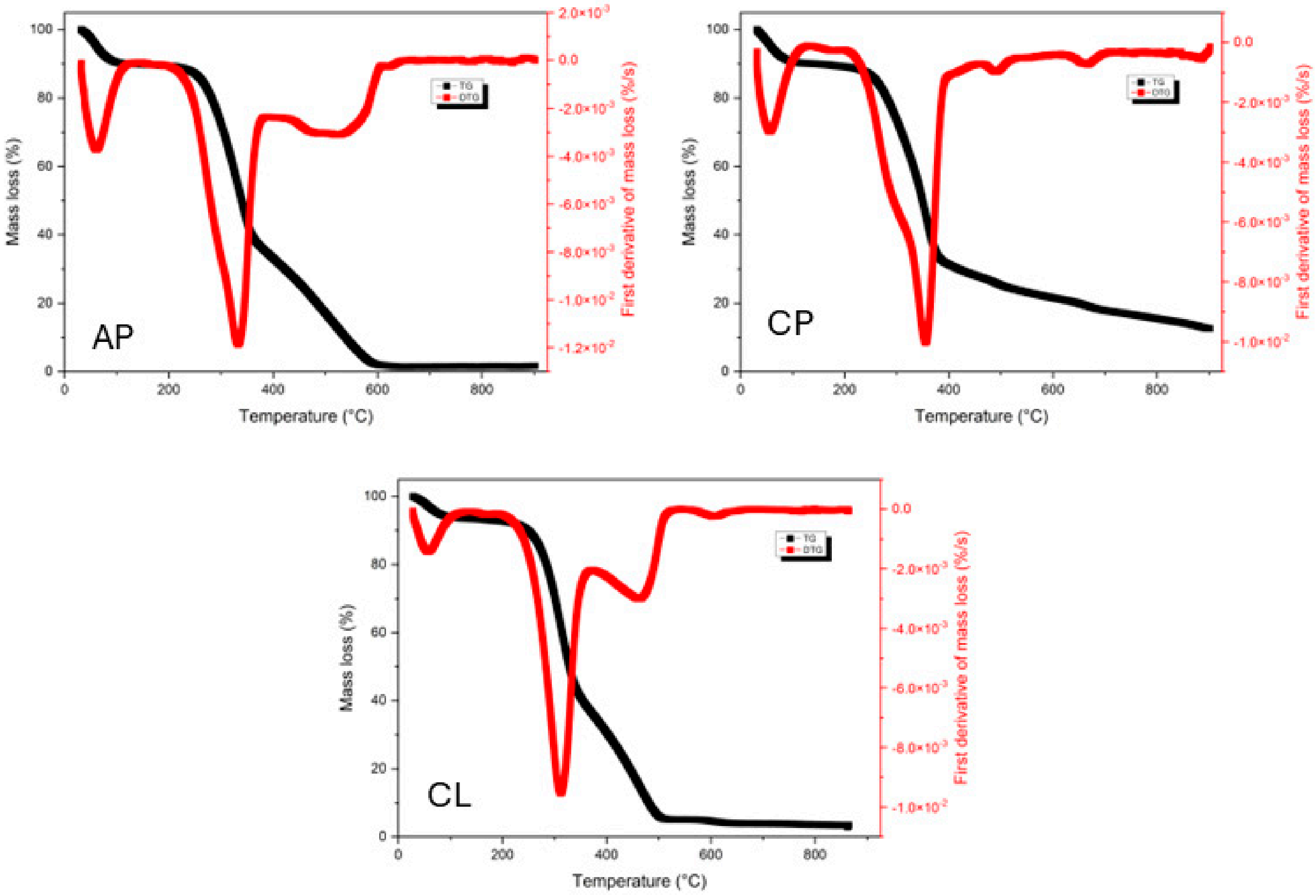

Figure 1. Temperature-dependent mass loss and rate of mass loss profiles recorded during the thermal decomposition of three wood residues.

The ash content corresponds to minerals absorbed during biomass growth, forming the inorganic part post-burning, and its chemical composition is influenced by the soil during biomass growth. As an inherent characteristic, soils in Northeast Brazil's semi-arid region exhibit considerable levels of nutrients, including calcium (Ca) and potassium (K) [46,47]. Hence, the high content of CaO and K_2O in the inorganic matter (ash) of three wood residues is justified, whereas elements like Fe_2O_3 and SiO_2 were observed in lower amounts. As indicated in Table 1, calcium is the prevalent mineral observed in the chemical composition of the ashes from AP and CP wood residues. In contrast, potassium is the prevalent mineral exhibited in the chemical composition of the ashes of CL wood residue. One plausible explanation is the more facile absorption and fixation of nutrient K from the soil by CL trees. The catalytic action mechanism of biomass ashes is elucidated in the literature, wherein alkaline and alkaline earth metals are found to form complexes with hydroxyl and/or phenolic groups inherent in the macromolecular structure of biomass [48,49]. Literature investigations have furnished evidence that the complexation of these cations within the cellulose structure facilitates scission in the polymeric chain, leading to the production of smaller compounds, such as furan derivatives and short-chain oxygenated compounds (C_1–C_4), instead of levoglucosan [50,51].

Favorable HHV values are demonstrated by wood residues derived from suppressed native species (Table 1), with the following order: AP (18.39 MJ kg^{-1}) > CL (17.99 MJ kg^{-1}) > CP (17.47 MJ kg^{-1}). The energy content of the three wood residues closely aligns with published values for other wood species from the Brazilian semi-arid region (17.9–20.5 MJ kg^{-1}) [41]. Competing equivalently with the reported values for commonly used lignocellulosic materials in commercial-scale solid biofuels, which typically have potential energy values ranging from 14.6 to 19.4 MJ kg^{-1} [34], the herein demonstrated HHV values underscore the promising potential of wood residues derived from suppressed native species as a valuable feedstock for bioenergy applications.

Bulk density is practical in formulating an effective logistics strategy for biomass handling, storage, and transportation [52]. Higher bulk density values are anticipated to correlate with reduced storage, transportation, and handling costs. As indicated in Table 1, the studied wood residues exhibited the following bulk density order: AP (268.70 kg m^{-3}) > CP (237.10 kg m^{-3}) > CL (126.50 kg m^{-3}). Bulk densities for typical lignocellulosic biomass utilized for bioenergy purposes, such as pinus wood, rice husk, and sugarcane bagasse, were reported as 176 kg m^{-3}, 129 kg m^{-3}, and 119 kg m^{-3}, respectively [53–55]. These values were higher than or comparable to those observed for the wood residues characterized in this study. An additional crucial consideration related to handling and transportation is the energy density (LHV per unit volume), reflecting the available potential energy concerning the biomass volume. A high energy density has been demonstrated in AP and CP wood residues, with values of 4.92 and 4.14 GJ m^{-3}, respectively, in contrast to CL wood residue, which exhibits a lower density of 2.28 GJ m^{-3}. These values were observed to be competitive with those typical of lignocellulosic biomass used for bioenergy, such as rice husk (3.40 GJ m^{-3}), coffee wastes (4.41 GJ m^{-3}), sugarcane bagasse (1.80 GJ m^{-3}), bamboo cellulose pulp (2.77 GJ m^{-3}), and maize wastes (2.85 GJ m^{-3}) [56]. Therefore, the wood residues derived from suppressed native species can be presumed to be promising feedstocks for bioenergy purposes.

While the bulk density of wood residues derived from suppressed native species is higher than or comparable to other well-known biomass residues, it is noted that these residues are not competitive with densified biomass in the form of pellets and briquettes (350–750 kg m^{-3}) [57]. This disparity may pose a significant practical barrier to the large-scale application of these underexplored lignocellulosic residues for bioenergy purposes. One well-established approach is the utilization of densification processes to produce a highly densified solid biofuel that complies with standard specifications for solid fuels [58,59]. Through the conversion of wood residues in sawdust form into pellets or briquettes, an anticipated enhancement in bulk density (and consequently energy density) is expected to be achieved at a competitive level. Following densification, the anticipated outcome is the production of solid biofuel suitable as a competitive feedstock for industrial- or medium-sized domestic biomass burners serving bioenergy purposes. In this context, recommendations for future research involve conducting studies on densification processes, such as pelletization and briquetting, to broaden the potential applications of wood residues derived from suppressed native species in the field of bioenergy.

3.2. Examining the Potential for Producing Renewable Chemicals

Figure 2 depicts the distribution of volatile reaction products released from three wood biomasses when subjected to flash pyrolysis, categorized by their chemical class. The volatile reaction products, subjected to analysis through the GC/MS system, were classified into primary categories determined by their organic functional groups. These categories include lighter oxygenated compounds (C_1–C_4), acetic acid, furan derivatives, phenolic compounds, cyclic ketones, other oxygenated cyclic compounds, alkanes, and unidentified compounds (with similarity scores below 85%). Table 2 displays the compounds identified in the volatile reaction products resulting from the flash pyrolysis of the three wood biomasses, including their molecular formula, molecular weight, and relative concentration, in which a predominance of oxygenated products is evident.

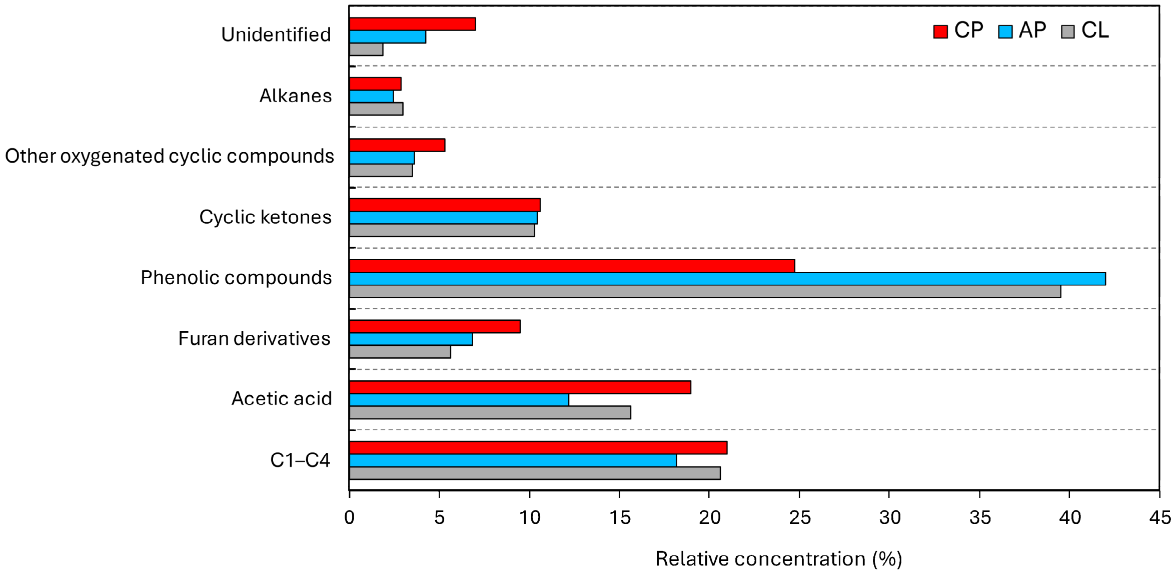

Figure 2. Distribution of volatile reaction products arising from three wood residues when subjected to flash pyrolysis, categorized according to their chemical class.

Table 2. Identified volatile reaction products from the three wood residues when subjected to flash pyrolysis.

Compound	Molecular Formula	Molecular Weight	Relative Concentration (%)		
			AP	CP	CL
C_1–C_4	–	–	18.19	20.98	20.59
Acetic acid			12.19	18.96	15.63
1,3–Dioxane	$C_4H_8O_2$	88	3.62	2.94	2.55
Unknown	–	–	4.25	7.00	1.89
3–Furaldehyde	$C_5H_4O_2$	96	3.29	4.30	3.07
2–Furanmethanol	$C_5H_6O_2$	98	3.57	5.18	2.54
Cyclopentanone	C_5H_8O	84	2.07	2.33	2.20
2–Hydroxy–2–cyclopenten–1–one	$C_5H_6O_2$	98	4.84	5.27	4.25
Phenol	C_6H_6O	94	–	–	3.68
2–Hydroxy–3–methyl–2–cyclopenten–1–one	$C_6H_8O_2$	112	2.91	2.10	2.94
4–Methylphenol	C_7H_8O	108	–	–	2.48
Mequinol	$C_7H_8O_2$	124	8.36	3.19	2.48
2,7–Dimethyl–octane	$C_{10}H_{22}$	142	2.44	2.88	2.98
2–Hydroxy–3,5–dimethylcyclopent–2–en–1–one	$C_7H_{10}O_2$	126	0.62	0.93	0.92
2–Methoxy–5–methylphenol	$C_8H_{10}O_2$	138	7.48	3.08	3.29
4–Ethyl–2–methoxyphenol	$C_9H_{12}O_2$	152	2.44	0.82	1.81
2–Methoxy–4–vinylphenol	$C_9H_{10}O_2$	150	10.48	6.07	11.59
2,6–Dimethoxyphenol	$C_8H_{10}O_3$	154	2.30	5.60	6.99
Eugenol	$C_{10}H_{10}O_2$	164	2.34	1.12	1.09
2–Methoxy–4–(1–propenyl)–phenol	$C_{10}H_{12}O_2$	164	1.33	0.65	0.85
1,2,4–Trimethoxybenzene	$C_9H_{12}O_3$	168	–	2.39	0.96
2–Methoxy–6–(2–propenyl)–phenol	$C_{10}H_{12}O_2$	164	7.28	4.23	5.23

The volatile reaction products, including short-chain oxygenated compounds (C_1–C_4), acetic acid, furan derivatives, cyclic ketones, other oxygenated cyclic compounds, and alkanes, observed from the three wood residues during flash pyrolysis, can be attributed to the thermal decomposition of cellulose and hemicellulose. Literature investigations yielded evidence that supports this hypothesis [38–40]. As illustrated in Figure 2, the class of short-chain oxygenated compounds (C_1–C_4) constituted the second-largest proportion of the volatile reaction products, exhibiting the following order: CP (20.98%) > CL (20.59%) > AP (18.19%). A unique hydrocarbon, 2,7-dimethyl-octane, was identified in the volatile pyrolysis products of wood residues from all three suppressed species, with its highest relative concentration

(3.0%) observed in the AP wood residue. The occurrence of 1,2,4–trimethoxybenzene, an oxygenated cyclic compound, in the volatile pyrolysis products derived from CP and CL wood residues, exhibits its maximum relative concentration (2.4%) in the CP wood residue and is commonly ascribed to the thermal decomposition of lignin [39].

As depicted in Figure 2, the acetic acid class constituted the third-largest proportion of the volatile reaction products, with the highest concentration observed in CP wood residue, accounting for approximately 19.0% of all volatile reaction products. This is a significant yield in comparison with acetic acid yields obtained from the pyrolysis of typical lignocellulosic biomass previously used for bio-oil production, including cherry wood (11.5%), olive wood (9.1%), hazelnut shell (12.4%), corn cobs (15.1%), almond shells (15.4%), and corn stalks (14.7%) [60]. Considering these findings and the potential applications of volatile reaction products into the condensable form (bio-oil) from the flash pyrolysis of CP wood residue, the extraction of compounds like acetic acid can be conceivable. Acetic acid, a valuable industrial chemical, is mainly utilized as a solvent owing to its exceptional solubility and miscibility. Furthermore, it is a crucial chemical raw material widely used in agriculture, medicine, textiles, adhesives, cosmetics, food, and other fields [61]. Another significant application lies in its role as a raw material for synthesizing cellulose acetate/polyvinyl acetate polymers and its importance as an acidity regulator in various chemical processes [60,61].

Furan derivatives, including 3–furaldehyde and 2–furan methanol, were identified among the volatile reaction products from the three wood residues, with the highest content observed in CP wood residue, constituting approximately 9.5% of all volatile reaction products. Furan derivatives serve as an important platform chemical employed in the chemical industry for various applications, including use as a solvent, alcohol, resin precursor, or intermediate in producing fragrances, C vitamins, and herbicides [40]. The main products from the thermal decomposition of cellulose, levoglucosan, and its derivatives were not detected among the volatile reaction products of the three wood residues. One possible explanation is that the alkaline metals, including K^+ and Ca^{2+} present in biomass ash, act as natural catalysts, altering the cellulose depolymerization pathway and leading to the formation of products such as furan derivatives and short-chain oxygenated compounds (C_1–C_4) instead of levoglucosan. Literature investigations provided corroborative evidence for this assertion [50,51]. Also, the release of furan derivatives may be associated with secondary reactions involving levoglucosan, potentially catalyzed by alkali metals present in biomass ash [40].

Phenolic compounds, which primarily originate from the thermal decomposition of lignin [40,62], constituted the prevalent constituents among the resulting volatile reaction products from the analytical flash pyrolysis of each of the three lignocellulosic biomasses, as demonstrated in Table 2. As expected, the differences in the lignocellulosic chemical composition led to distinct relative concentrations of phenolic compounds: CL and AP wood residues, with higher lignin percentages in their compositions, exhibited the highest relative phenolic compound concentrations (40%–42%), whereas CP, with the lowest lignin content, displayed the lowest relative phenolic compound concentration (27%). It is well-known that the elevated molecular weight and viscosity of bio-oils are primarily attributed to lignin-derived products [62]. Also, phenolic compounds, classified as aromatic oxygenated compounds, may adversely impact bio-oil when intended for use as fuel due to oxidation reactions, imparting a degree of instability [63]. Despite the drawbacks associated with the presence of phenolic compounds, recent studies have emphasized that phenolic-rich bio-oil demonstrates insecticidal properties, a positive attribute [23,64].

According to the literature, phenolic compounds are classified into four categories based on aromatic substituent groups: the guaiacol type (G–), the phenol type (H–), the syringol type (S–), and the catechol type (C–) [65,66]. The distribution of phenolic products, categorized by their aromatic substituent groups and resulting from the flash pyrolysis of three wood residues, is illustrated in Figure 3. Hence, it is inferred that the volatile products derived from the thermal decomposition of lignin primarily consisted of monoaromatic phenolic compounds, predominantly associated with hydroxyl and methoxyl groups. The G–type phenols were the predominant group, in contrast to the H– and S–types, with the highest proportion provided by CP wood residue. The predominant G–type phenolic compounds, delineated by their relative concentrations from the three wood residues, include 2–methoxy–5–methylphenol, 2–methoxy–4–vinylphenol, and 2–methoxy–6–(2–propenyl)–phenol. Within the G–phenolic compounds, 2–methoxy–4–vinylphenol emerged with the highest relative concentration. This phenolic compound holds industrial significance, as it serves as a flavoring agent in the food industry and finds applications in synthesizing resins and pharmaceuticals [67]. In contrast, phenol and 4–methylphenol emerged as the sole products among the H–type phenolic compounds, while 2,6–dimethoxyphenol stood out as the exclusive product among the S–type phenolic compounds. The formation of S–type phenolic compounds (containing two $-OCH_3$) is attributed to the cleavage of syringyl groups within the lignin macromolecule [39].

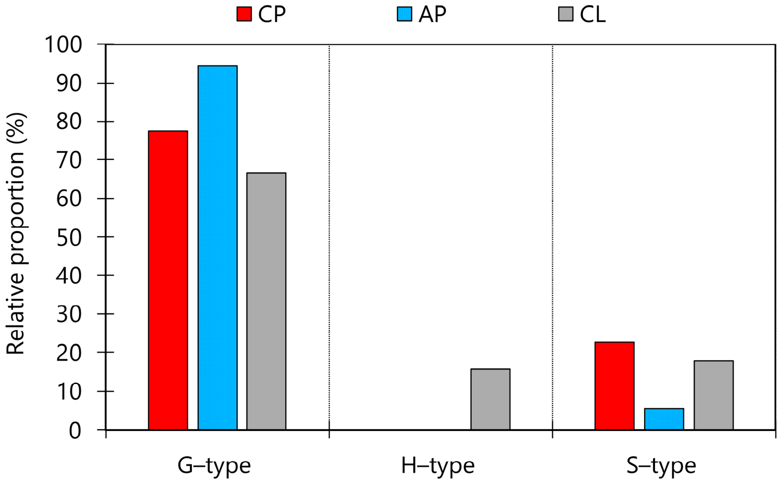

Figure 3. Distribution of phenolic products arising from three wood residues when subjected to flash pyrolysis, categorized according to their aromatic substituent groups.

The prevalence of G–type phenolic compounds (methoxy groups indicates) indicates the predominance of the guaiacyl unit in the alkali lignin. G–type phenolic compounds can be produced through the direct cleavage of the β–O–4 bond, which possesses the lowest dissociation energy among all linkage bonds [65]. *Cenostigma pyramidale* belongs to the family Fabaceae, *Commiphora leptophloeos* belongs to the family Burseraceae, and *Aspidosperma pyrifolium* belongs to the family Apocynaceae; all are classified as Angiospermae families [68,69]. The term "hardwood' is frequently employed to denote the extensive category of angiosperm trees, and this distinction is crucial as the characteristics of phenolic compounds depend on whether a "hardwood" or "softwood" species is subjected to pyrolysis [70]. While guaiacols and syringols form hardwood lignin in comparable proportions [70,71], a predominance of G–type phenolic compounds was observed in the flash pyrolysis of three wood residues, as opposed to S–type phenolic compounds. One possible explanation for the observed phenomenon is the demethoxylation reactions, which progressively convert S–type phenolic compounds into G–type phenolic compounds through $O-CH_3$ bond homolysis. This decomposition leads to the production of phenol, cresol, and catechol at temperatures above 400 °C [72,73]. Literature investigations yielded similar observations to those found in this case study [74], corroborating the results obtained.

In light of the encouraging outcomes observed in this case study, the transition of flash pyrolysis applied to the studied wood residues to a commercial scale is recommended, driven by its potential capacity to generate bio-oil rich in valuable phenolic compounds. The flash pyrolysis of wood residues derived from suppressing native species can be viewed as an alternative approach to replace fossil-based counterparts in producing phenolic compounds. This is particularly relevant for sustainability and aligns with potential applications in green chemistry scenarios. In recent literature, phenolic compounds have been emphasized for their value in various industrial applications. For example, 2,6–dimethoxyphenol is used in the production of synthetic smoke flavorings, and 2–methoxy–4–vinylphenol is recognized as an aromatic substance frequently employed as a flavoring agent, contributing to the natural aroma of buckwheat [75]. Furthermore, producing bio-oil rich in phenolic compounds allows for its subsequent use in producing phenol-formaldehyde resins, thereby diminishing reliance on petroleum-derived phenols in resin manufacturing [76]. Other relevant industrial applications for phenolic compounds include their use as additives in the fertilizing and pharmaceutical industries, as flavoring agents in the food industry, and their utility in preparing dyes, explosives, lubricants, pesticides, and plastics [76–78]. In summary, the valorization of wood residues resulting from suppressing native species through flash pyrolysis can reduce the environmental impacts associated with wind energy plant installation. This valorization route yields phenolic compounds with substantial applicative potential, contributing to the bioeconomy and concurrently aligning with Sustainable Development Goals (SDGs) 7, 9, 13, and 15 targets.

4. Conclusions

This pioneering study proposes valorizing CP, CL, and AP wood residues from suppressing native species within the caatinga biome during wind energy plant installation. Notably, AP wood residue is identified as the preferred feedstock for bioenergy production, exhibiting superior characteristics in terms of bulk density, HHV, and ash content. While the energy-related properties indicating the potential value of three wood residues as energy resources are apparent, their bulk density is not competitive with densified biomass in pellet and briquette forms. This may pose a significant obstacle to the large-scale utilization of these wood residues for energy purposes. Hence, it is recommended to improve their suitability for the bioenergy sector by densifying them into solid biofuels through pelleting or briquetting, ensuring they meet the standard specifications for solid fuels. Additionally, to enhance the utilization of wood residues resulting from suppressing native species within the caatinga biome during wind energy plant installation for bioenergy and renewable chemical production, a key technical consideration involves assessing the local availability of these resources. Consequently, future research may focus on estimating the biomass availability for bioenergy and renewable chemical production by suppressing native species in the caatinga biome during wind energy plant installations, taking into account site-specific factors such as wood yields, multi-annual yield variations, environmental constraints, and competitive uses.

This study also pioneers assessing phenolic-enriched bio-oil production potential from three wood residues resulting from vegetation suppression during wind energy plant installation. It involved screening the organic compounds in volatile reaction products from the flash pyrolysis of each wood residue by Py–GC/MS analysis. Phenolic compounds were identified as the dominant constituents in volatile pyrolysis products, implying favorable prospects for phenolic-enriched bio-oil production. The industrial significance of phenolic-enriched bio-oil is underscored, as it emerges as an appealing product across diverse sectors, encompassing industries such as paints, phenolic resins, and pesticides. Among the three wood residues, CL and AP wood residues show the highest potential for phenolic-enriched bio-oil production, with phenolic compound contents exceeding 40% in volatile flash pyrolysis products, attributed to their higher lignin content compared to CP wood residue. Also noteworthy is the elevated content of acetic acid, a highly relevant industrial chemical, in the volatile pyrolysis products derived from CP wood residue, with an estimated relative concentration of approximately 19.0%. Other renewable and high-value-added chemicals, such as ketones, furans, and ethers, can also be harvested from the volatile reaction products of the flash pyrolysis of three wood residues, albeit in minor proportions. The utilization of catalysts in the deoxygenation of volatile pyrolysis products, converting them into renewable hydrocarbons, results in the production of bio-oil capable of serving as a precursor for drop-in biofuels, such as green gasoline and bio-jet fuel, which are oxygen-free and functionally emulate petroleum fuels. This approach merits further exploration in future research endeavors.

Supplementary Materials: The following supporting information can be downloaded at: https://www.mdpi.com/article/10.3390/f15040621/s1, Figure S1: Location of the Jandaíra Wind Farm Project in the Mato Grande region; Figure S2: *Griffinia gardneriana* rescued from an area designated for vegetal suppression.

Author Contributions: Conceptualization, M.C.P.d.S.A., J.L.F.A. and R.M.B.; Methodology, M.C.P.d.S.A. and R.M.B.; Formal analysis, M.C.P.d.S.A. and R.M.B.; Investigation, M.C.P.d.S.A.; Resources, D.M.d.A.M. and A.S.P.; Data curation, M.C.P.d.S.A., J.E.d.S., W.G.d.S.B. and J.L.F.A.; Writing—original draft, M.C.P.d.S.A.; Writing—review & editing, J.L.F.A. and A.S.P.; Visualization, W.G.d.S.B., J.L.F.A. and A.S.P.; Supervision, D.M.d.A.M. and R.M.B.; Project administration, R.M.B. All authors have read and agreed to the published version of the manuscript.

Funding: This research was funded by Brazil's National Council for Scientific and Technological Development (CNPq/Process 307433/2020-0) and Brazil's Coordination for the Improvement of Higher Education Personnel (CAPES/Finance Code 001).

Data Availability Statement: The data presented in this study are available on request from the corresponding author.

Acknowledgments: The authors express their gratitude to LabTam-UFRN for the infrastructure made available to support the development of this study. The authors also acknowledge financial support from Brazil's National Council for Scientific and Technological Development.

Conflicts of Interest: All authors agree with the submission and declare no conflict of interest regarding the manuscript's content, ethical procedures, and funding agencies.

References

1. Salvia, A.L.; Brandli, L.L. *Energy Sustainability at Universities and Its Contribution to SDG 7: A Systematic Literature Review*; Springer International Publishing: Berlin/Heidelberg, Germany, 2020; ISBN 9783030156046.
2. Albanito, F.; Roberts, S.; Shepherd, A.; Hastings, A. Quantifying the Land-Based Opportunity Carbon Costs of Onshore Wind Farms. *J. Clean. Prod.* **2022**, *363*, 132480. [CrossRef]
3. Steffen, B.; Patt, A. A Historical Turning Point? Early Evidence on How the Russia-Ukraine War Changes Public Support for Clean Energy Policies. *Energy Res. Soc. Sci.* **2022**, *91*, 102758. [CrossRef]
4. Agaton, C.B. Will a Geopolitical Conflict Accelerate Energy Transition in Oil-Importing Countries? A Case Study of the Philippines from a Real Options Perspective. *Resources* **2022**, *11*, 59. [CrossRef]
5. Schneider, F.; Kallis, G.; Martinez-Alier, J. Crisis or Opportunity? Economic Degrowth for Social Equity and Ecological Sustainability. Introduction to This Special Issue. *J. Clean. Prod.* **2010**, *18*, 511–518. [CrossRef]
6. Khoshnava, S.M.; Rostami, R.; Zin, R.M.; Štreimikiene, D.; Yousefpour, A.; Strielkowski, W.; Mardani, A. Aligning the Criteria of Green Economy (GE) and Sustainable Development Goals (SDGs) to Implement Sustainable Development. *Sustainability* **2019**, *11*, 4615. [CrossRef]
7. Lima, M.A.; Mendes, L.F.R.; Mothé, G.A.; Linhares, F.G.; de Castro, M.P.P.; da Silva, M.G.; Sthel, M.S. Renewable Energy in Reducing Greenhouse Gas Emissions: Reaching the Goals of the Paris Agreement in Brazil. *Environ. Dev.* **2020**, *33*, 100504. [CrossRef]
8. Soares, M.C.; Borba, B.; Szklo, A.; Schaeffer, R. Plug-in Hybrid Electric Vehicles as a Way to Maximize the Integration of Variable Renewable Energy in Power Systems: The Case of Wind Generation in Northeastern Brazil. *Energy* **2012**, *37*, 469–481. [CrossRef]
9. Junior, M.F.S.; Hernandez, M.C.R.; Amora, S.S.A.; de Morais, E.R.C. Perception of Environmental Impacts of Wind Farms in Agricultural Areas of Northeast Brazil. *Energies* **2022**, *15*, 101. [CrossRef]
10. Ma, B.; Yang, J.; Chen, X.; Zhang, L.; Zeng, W. Revealing the Ecological Impact of Low-Speed Mountain Wind Power on Vegetation and Soil Erosion in South China: A Case Study of a Typical Wind Farm in Yunnan. *J. Clean. Prod.* **2023**, *419*, 138020. [CrossRef]
11. Solís-Chaves, J.S.; Rocha-Osorio, C.M.; Murari, A.L.L.; Lira, V.M.; Sguarezi Filho, A.J. Extracting Potable Water from Humid Air plus Electric Wind Generation: A Possible Application for a Brazilian Prototype. *Renew. Energy* **2018**, *121*, 102–115. [CrossRef]
12. Urziceanu, M.; Anastasiu, P.; Rozylowicz, L.; Sesan, T.E. Local-Scale Impact of Wind Energy Farms on Rare, Endemic, and Threatened Plant Species. *PeerJ* **2021**, *9*, e11390. [CrossRef] [PubMed]
13. Cunningham, S.C.; Mac Nally, R.; Baker, P.J.; Cavagnaro, T.R.; Beringer, J.; Thomson, J.R.; Thompson, R.M. Balancing the Environmental Benefits of Reforestation in Agricultural Regions. *Perspect. Plant Ecol. Evol. Syst.* **2015**, *17*, 301–317. [CrossRef]
14. Bach, Q.-V.; Tran, K.-Q.; Skreiberg, Ø. Combustion Kinetics of Wet-Torrefied Forest Residues Using the Distributed Activation Energy Model (DAEM). *Appl. Energy* **2017**, *185*, 1059–1066. [CrossRef]

15. Ahmad, M.S.; Liu, C.-G.; Nawaz, M.; Tawab, A.; Shen, X.; Shen, B.; Mehmood, M.A. Elucidating the Pyrolysis Reaction Mechanism of Calotropis Procera and Analysis of Pyrolysis Products to Evaluate Its Potential for Bioenergy and Chemicals. *Bioresour. Technol.* **2021**, *322*, 124545. [CrossRef] [PubMed]
16. Alhumade, H.; Alayed, O.S.; Iqbal, M.W.; Shahid, A.; Iqbal, T.; Ahmad, M.S.; Elkamel, A.; Al-Turki, Y.; Mehmood, M.A.; Ashraf, G.A. Exploration of the Bioenergy Potential of Dactyloctenium Aegyptium through Pyrolysis, Kinetics, and Thermodynamic Parameters to Produce Clean Fuels and Biochemicals. *Fuel* **2023**, *341*, 127663. [CrossRef]
17. Tagade, A.; Kirti, N.; Sawarkar, A.N. Pyrolysis of Agricultural Crop Residues: An Overview of Researches by Indian Scientific Community. *Bioresour. Technol. Rep.* **2021**, *15*, 100761. [CrossRef]
18. Yao, Z.; Yu, S.; Su, W.; Wu, W.; Tang, J.; Qi, W. Kinetic Studies on the Pyrolysis of Plastic Waste Using a Combination of Model-Fitting and Model-Free Methods. *Waste Manag. Res.* **2020**, *38*, 77–85. [CrossRef]
19. Gupta, G.K.; Mondal, M.K. Kinetics and Thermodynamic Analysis of Maize Cob Pyrolysis for Its Bioenergy Potential Using Thermogravimetric Analyzer. *J. Therm. Anal. Calorim.* **2019**, *137*, 1431–1441. [CrossRef]
20. Azizi, S.; Mowla, D. CFD Modeling of Algae Flash Pyrolysis in the Batch Fluidized Bed Reactor Including Heat Carrier Particles. *Int. J. Chem. React. Eng.* **2016**, *14*, 463–480. [CrossRef]
21. Xiu, S.; Shahbazi, A. Bio-Oil Production and Upgrading Research: A Review. *Renew. Sustain. Energy Rev.* **2012**, *16*, 4406–4414. [CrossRef]
22. Iha, O.K.; Alves, F.C.S.C.; Suarez, P.A.Z.; de Oliveira, M.B.F.; Meneghetti, S.M.P.; Santos, B.P.T.; Soletti, J.I. Physicochemical Properties of Syagrus Coronata and Acrocomia Aculeata Oils for Biofuel Production. *Ind. Crops Prod.* **2014**, *62*, 318–322. [CrossRef]
23. Tahir, M.H.; Irfan, R.M.; Cheng, X.; Ahmad, M.S.; Jamil, M.; Shah, T.U.H.; Karim, A.; Ashraf, R.; Haroon, M. Mango Peel as Source of Bioenergy, Bio-Based Chemicals via Pyrolysis, Thermodynamics and Evolved Gas Analyses. *J. Anal. Appl. Pyrolysis* **2021**, *155*, 105066. [CrossRef]
24. Mishra, R.K.; Mohanty, K.; Wang, X. Pyrolysis Kinetic Behavior and Py-GC–MS Analysis of Waste Dahlia Flowers into Renewable Fuel and Value-Added Chemicals. *Fuel* **2020**, *260*, 116338. [CrossRef]
25. Pal, S.K.; Garcés-Sánchez, G.; Kranert, M.; Vinu, R. Characterization and Evaluation of Resource Recovery Potential of Beach Plastic Wastes Using Analytical Py-GC/MS. *J. Anal. Appl. Pyrolysis* **2023**, *172*, 105996. [CrossRef]
26. Qiao, Y.; Wang, B.; Zong, P.; Tian, Y.; Xu, F.; Li, D.; Li, F.; Tian, Y. Thermal Behavior, Kinetics and Fast Pyrolysis Characteristics of Palm Oil: Analytical TG-FTIR and Py-GC/MS Study. *Energy Convers. Manag.* **2019**, *199*, 111964. [CrossRef]
27. *ASTM E871-82*; Standard Test Method for Moisture Analysis of Particulate Wood Fuels. ASTM International: West Conshohocken, PA, USA, 2019.
28. *ASTM E872-82*; Standard Test Method for Volatile Matter in the Analysis of Particulate Wood Fuels. ASTM International: West Conshohocken, PA, USA, 2019.
29. *ASTM E1755-01*; Standard Test Method for Ash in Biomass. ASTM International: West Conshohocken, PA, USA, 2010.
30. Correia, L.A.d.S.; da Silva, J.E.; Calixto, G.Q.; Melo, D.M.d.A.; Braga, R.M. Pachira Aquatica Fruits Shells Valorization: Renewables Phenolics through Analytical Pyrolysis Study (Py-GC/MS). *Cienc. Rural* **2022**, *52*, 1–11. [CrossRef]
31. Van Soest, P.J.; Robertson, J.B.; Lewis, B.A. Methods for Dietary Fiber, Neutral Detergent Fiber, and Nonstarch Polysaccharides in Relation to Animal Nutrition. *J. Dairy Sci.* **1991**, *74*, 3583–3597. [CrossRef]
32. *ASTM E873-82*; Standard Test Method for Bulk Density of Densified Particulate Biomass Fuels. ASTM International: West Conshohocken, PA, USA, 2013.
33. García, R.; Pizarro, C.; Lavín, A.G.; Bueno, J.L. Biomass Sources for Thermal Conversion. Techno-Economical Overview. *Fuel* **2017**, *195*, 182–189. [CrossRef]
34. García, R.; Pizarro, C.; Lavín, A.G.; Bueno, J.L. Spanish Biofuels Heating Value Estimation. Part I: Ultimate Analysis Data. *Fuel* **2014**, *117*, 1130–1138. [CrossRef]
35. Yang, Y.B.; Ryu, C.; Khor, A.; Yates, N.E.; Sharifi, V.N.; Swithenbank, J. Effect of Fuel Properties on Biomass Combustion. Part II. Modelling Approach—Identification of the Controlling Factors. *Fuel* **2005**, *84*, 2116–2130. [CrossRef]
36. Díez, D.; Urueña, A.; Piñero, R.; Barrio, A.; Tamminen, T. Determination of Hemicellulose, Cellulose, and Lignin Content in Different Types of Biomasses by Thermogravimetric Analysis and Pseudocomponent Kinetic Model (TGA-PKM Method). *Processes* **2020**, *8*, 1048. [CrossRef]
37. Geng, W.; Narron, R.; Jiang, X.; Pawlak, J.J.; Chang, H.m.; Park, S.; Jameel, H.; Venditti, R.A. The Influence of Lignin Content and Structure on Hemicellulose Alkaline Extraction for Non-Wood and Hardwood Lignocellulosic Biomass. *Cellulose* **2019**, *26*, 3219–3230. [CrossRef]
38. Bertero, M.; de la Puente, G.; Sedran, U. Fuels from Bio-Oils: Bio-Oil Production from Different Residual Sources, Characterization and Thermal Conditioning. *Fuel* **2012**, *95*, 263–271. [CrossRef]
39. Subagyono, R.D.J.N.; Miten, P.D.; Sinaga, R.J.; Wijayanti, A.; Qi, Y.; Marshall, M.; Sanjaya, A.S.; Chaffee, A.L. Pyrolysis of Fast Growing Wood Macaranga Gigantea: Product Characterisation and Kinetic Study. *Fuel* **2022**, *315*, 123182. [CrossRef]
40. Braga, R.M.; Melo, D.M.A.; Melo, M.A.F.; Freitas, J.C.O.; Boateng, A.A. Effect of Pretreatment on Pyrolysis Products of Pennisetum Purpureum Schum. by Py-GC/MS. *J. Therm. Anal. Calorim.* **2022**, *147*, 6655–6663. [CrossRef]
41. Dias Júnior, A.F.; Andrade, C.R.; Protásio, T.D.P.; Brito, J.O.; Trugilho, P.F.; Oliveira, M.P.; Dambroz, G.B.V. Thermal Profile of Wood Species from the Brazilian Semi-Arid Region Submitted to Pyrolysis. *Cerne* **2019**, *25*, 44–53. [CrossRef]

42. Aboyade, A.O.; Hugo, T.J.; Carrier, M.; Meyer, E.L.; Stahl, R.; Knoetze, J.H.; Görgens, J.F. Non-Isothermal Kinetic Analysis of the Devolatilization of Corn Cobs and Sugar Cane Bagasse in an Inert Atmosphere. *Thermochim. Acta* **2011**, *517*, 81–89. [CrossRef]
43. Ma, Z.; Chen, D.; Gu, J.; Bao, B.; Zhang, Q. Determination of Pyrolysis Characteristics and Kinetics of Palm Kernel Shell Using TGA-FTIR and Model-Free Integral Methods. *Energy Convers. Manag.* **2015**, *89*, 251–259. [CrossRef]
44. Pinzi, S.; Buratti, C.; Bartocci, P.; Marseglia, G.; Fantozzi, F.; Barbanera, M. A Simplified Method for Kinetic Modeling of Coffee Silver Skin Pyrolysis by Coupling Pseudo-Components Peaks Deconvolution Analysis and Model Free-Isoconversional Methods. *Fuel* **2020**, *278*, 118260. [CrossRef]
45. Gupta, S.; Gupta, G.K.; Mondal, M.K. Thermal Degradation Characteristics, Kinetics, Thermodynamic, and Reaction Mechanism Analysis of Pistachio Shell Pyrolysis for Its Bioenergy Potential. *Biomass Convers. Biorefinery* **2020**, *12*, 4847–4861. [CrossRef]
46. da Rocha Mendes, K.; Portela, J.C.; Gondim, J.E.F.; Ribeiro, M.A.; de Medeiros, J.F.; de Queiroz, G.C.M. Physical, Chemical and Structural Attributes of Soil in Agroecosystems in the Brazilian Semiarid Region. *Rev. Cienc. Agron.* **2022**, *53*, 1–10. [CrossRef]
47. de Paiva, K.F.; Severo, P.J.d.S.; de Oliveira, F.S.; Soares, L.A.D.A.; Araujo, J.L. Potassium Availability in Brazilian Semiarid Soils Cultivated with Melon. *Pesqui. Agropecu. Trop.* **2020**, *50*, 1–8. [CrossRef]
48. Mahadevan, R.; Adhikari, S.; Shakya, R.; Wang, K.; Dayton, D.; Lehrich, M.; Taylor, S.E. Effect of Alkali and Alkaline Earth Metals on In-Situ Catalytic Fast Pyrolysis of Lignocellulosic Biomass: A Microreactor Study. *Energy Fuels* **2016**, *30*, 3045–3056. [CrossRef]
49. Nik-Azar, M.; Hajaligol, M.R.; Sohrabi, M.; Dabir, B. Mineral Matter Effects in Rapid Pyrolysis of Beech Wood. *Fuel Process. Technol.* **1997**, *51*, 7–17. [CrossRef]
50. Patwardhan, P.R.; Satrio, J.A.; Brown, R.C.; Shanks, B.H. Influence of Inorganic Salts on the Primary Pyrolysis Products of Cellulose. *Bioresour. Technol.* **2010**, *101*, 4646–4655. [CrossRef]
51. Collard, F.X.; Blin, J.; Bensakhria, A.; Valette, J. Influence of Impregnated Metal on the Pyrolysis Conversion of Biomass Constituents. *J. Anal. Appl. Pyrolysis* **2012**, *95*, 213–226. [CrossRef]
52. Cai, J.; He, Y.; Yu, X.; Banks, S.W.; Yang, Y.; Zhang, X.; Yu, Y.; Liu, R.; Bridgwater, A.V. Review of Physicochemical Properties and Analytical Characterization of Lignocellulosic Biomass. *Renew. Sustain. Energy Rev.* **2017**, *76*, 309–322. [CrossRef]
53. Kumar, M.; Upadhyay, S.N.; Mishra, P.K. A Comparative Study of Thermochemical Characteristics of Lignocellulosic Biomasses. *Bioresour. Technol. Rep.* **2019**, *8*, 100186. [CrossRef]
54. Abdullah, M.Z.; Husain, Z.; Yin Pong, S.L. Analysis of Cold Flow Fluidization Test Results for Various Biomass Fuels. *Biomass Bioenergy* **2003**, *24*, 487–494. [CrossRef]
55. Lenis, Y.A.; Osorio, L.F.; Pérez, J.F. Fixed Bed Gasification of Wood Species with Potential as Energy Crops in Colombia: The Effect of the Physicochemical Properties. *Energy Sources Part A Recovery Util. Environ. Eff.* **2013**, *35*, 1608–1617. [CrossRef]
56. Protásio, T.d.P.; Bufalino, L.; Tonoli, G.H.D.; Guimarães Junior, M.; Trugilho, P.F.; Mendes, L.M. Brazilian Lignocellulosic Wastes for Bioenergy Production: Characterization and Comparison with Fossil Fuels. *BioResources* **2013**, *8*, 1166–1185. [CrossRef]
57. Tumuluru, J.S. Effect of Pellet Die Diameter on Density and Durability of Pellets Made from High Moisture Woody and Herbaceous Biomass. *Carbon Resour. Convers.* **2018**, *1*, 44–54. [CrossRef]
58. Olugbade, T.; Ojo, O.; Mohammed, T. Influence of Binders on Combustion Properties of Biomass Briquettes: A Recent Review. *BioEnergy Res.* **2019**, *12*, 241–259. [CrossRef]
59. de Souza, H.J.P.L.; Arantes, M.D.C.; Vidaurre, G.B.; Andrade, C.R.; de Cássia Oliveira Carneiro, A.; de Souza, D.P.L.; de Paula Protásio, T. Pelletization of Eucalyptus Wood and Coffee Growing Wastes: Strategies for Biomass Valorization and Sustainable Bioenergy Production. *Renew. Energy* **2020**, *149*, 128–140. [CrossRef]
60. Sarchami, T.; Batta, N.; Berruti, F. Production and Separation of Acetic Acid from Pyrolysis Oil of Lignocellulosic Biomass: A Review. *Biofuels Bioprod. Biorefining* **2021**, *15*, 1912–1937. [CrossRef]
61. Chen, Y.; Yang, Y.; Liu, X.; Shi, X.; Wang, C.; Zhong, H.; Jin, F. Sustainable Production of Formic Acid and Acetic Acid from Biomass. *Mol. Catal.* **2023**, *545*, 113199. [CrossRef]
62. Veses, A.; Aznar, M.; López, J.M.; Callén, M.S.; Murillo, R.; García, T. Production of Upgraded Bio-Oils by Biomass Catalytic Pyrolysis in an Auger Reactor Using Low Cost Materials. *Fuel* **2015**, *141*, 17–22. [CrossRef]
63. Chagas, B.M.E.; Dorado, C.; Serapiglia, M.J.; Mullen, C.A.; Boateng, A.A.; Melo, M.A.F.; Ataíde, C.H. Catalytic Pyrolysis-GC/MS of Spirulina: Evaluation of a Highly Proteinaceous Biomass Source for Production of Fuels and Chemicals. *Fuel* **2016**, *179*, 124–134. [CrossRef]
64. Urrutia, R.I.; Yeguerman, C.; Jesser, E.; Gutierrez, V.S.; Volpe, M.A.; Werdin González, J.O. Sunflower Seed Hulls Waste as a Novel Source of Insecticidal Product: Pyrolysis Bio-Oil Bioactivity on Insect Pests of Stored Grains and Products. *J. Clean. Prod.* **2021**, *287*, 125000. [CrossRef]
65. Ma, Z.; Sun, Q.; Ye, J.; Yao, Q.; Zhao, C. Study on the Thermal Degradation Behaviors and Kinetics of Alkali Lignin for Production of Phenolic-Rich Bio-Oil Using TGA–FTIR and Py–GC/MS. *J. Anal. Appl. Pyrolysis* **2016**, *117*, 116–124. [CrossRef]
66. Kaur, R.; Tarun Kumar, V.; Krishna, B.B.; Bhaskar, T. Characterization of Slow Pyrolysis Products from Three Different Cashew Wastes. *Bioresour. Technol.* **2023**, *376*, 128859. [CrossRef] [PubMed]
67. da Silva, J.C.G.; Pereira, J.L.C.; Andersen, S.L.F.; Moreira, R.d.F.P.M.; José, H.J. Torrefaction of Ponkan Peel Waste in Tubular Fixed-Bed Reactor: In-Depth Bioenergetic Evaluation of Torrefaction Products. *Energy* **2020**, *210*, 118569. [CrossRef]
68. Menezes, J.C.; Neto, O.C.C.; Azevedo, I.F.P.; Machado, A.O.; Nunes, Y.R.F. Soil Seed Bank at Different Depths and Light Conditions in a Dry Forest in Northern Minas Gerais. *Floresta Ambient.* **2019**, *26*, 1–9. [CrossRef]

69. Vamosi, S.M. A Reconsideration of the Reproductive Biology of the Atlantic Forest in the Volta Velha Reserve. *Biodivers. Conserv.* **2006**, *15*, 1417–1424. [CrossRef]
70. Mohan, D.; Pittman, C.U.; Steele, P.H. Pyrolysis of Wood/Biomass for Bio-Oil: A Critical Review. *Energy Fuels* **2006**, *20*, 848–889. [CrossRef]
71. Kim, J.S. Production, Separation and Applications of Phenolic-Rich Bio-Oil—A Review. *Bioresour. Technol.* **2015**, *178*, 90–98. [CrossRef]
72. Shen, D.K.; Gu, S.; Luo, K.H.; Wang, S.R.; Fang, M.X. The Pyrolytic Degradation of Wood-Derived Lignin from Pulping Process. *Bioresour. Technol.* **2010**, *101*, 6136–6146. [CrossRef]
73. Asmadi, M.; Kawamoto, H.; Saka, S. Characteristics of Softwood and Hardwood Pyrolysis in an Ampoule Reactor. *J. Anal. Appl. Pyrolysis* **2017**, *124*, 523–535. [CrossRef]
74. Oliveira, G.P.D.; Araújo, L.; Siqueira, D.M.; Quintela, G.; Maria, D.; Melo, D.A.; Antonio, M.; Melo, D.F.; Pimenta, A.S.; Braga, R.M. Kinetic Study and Effect of Flash Pyrolysis Temperature of Kraft Lignin on the Yield of Aromatic Compounds. *J. Therm. Anal. Calorim.* **2023**, *148*, 12725–12737. [CrossRef]
75. Sobek, S.; Zeng, K.; Werle, S.; Junga, R.; Sajdak, M. Brewer's Spent Grain Pyrolysis Kinetics and Evolved Gas Analysis for the Sustainable Phenolic Compounds and Fatty Acids Recovery Potential. *Renew. Energy* **2022**, *199*, 157–168. [CrossRef]
76. Awasthi, A.; Dhyani, V.; Biswas, B.; Kumar, J.; Bhaskar, T. Production of Phenolic Compounds Using Waste Coir Pith: Estimation of Kinetic and Thermodynamic Parameters. *Bioresour. Technol.* **2019**, *274*, 173–179. [CrossRef]
77. Norouzi, O.; Jafarian, S.; Safari, F.; Tavasoli, A.; Nejati, B. Promotion of Hydrogen-Rich Gas and Phenolic-Rich Bio-Oil Production from Green Macroalgae Cladophora Glomerata via Pyrolysis over Its Bio-Char. *Bioresour. Technol.* **2016**, *219*, 643–651. [CrossRef]
78. Lazzari, E.; Schena, T.; Primaz, C.T.; da Silva Maciel, G.P.; Machado, M.E.; Cardoso, C.A.L.; Jacques, R.A.; Caramão, E.B. Production and Chromatographic Characterization of Bio-Oil from the Pyrolysis of Mango Seed Waste. *Ind. Crops Prod.* **2016**, *83*, 529–536. [CrossRef]